

Received June 1, 2020, accepted June 12, 2020, date of publication June 19, 2020, date of current version July 1, 2020.

Digital Object Identifier 10.1109/ACCESS.2020.3003722

Space Charge Transport Characteristic Considering the Non-Uniform Electric Effect of Ion Mobility

ZHAOXIANG ZHANG¹, KAI YANG¹, CHENG CHI¹, FAN YANG¹, (Member, IEEE), LI LIU², AND SHAOHUA WANG², (Member, IEEE)

¹State Key Laboratory of Power Transmission Equipment and System Security and New Technology, School of Electrical Engineering, Chongqing University—University of Cincinnati Joint Co-op Institute, Chongqing University, Chongqing 400044, China

²Electric Power Research Institute, State Grid Zhejiang Electric Power Company, Hangzhou 310007, China

Corresponding authors: Zhaoxiang Zhang (zhangzhaoxiang0210@foxmail.com) and Fan Yang (yangfancqu@gmail.com)

This work was supported in part by the National Key Research and Development Program under Grant 2017YFB0902703, and in part by the Science and Technology Project of State Grid Zhejiang Electric Power Company under Grant 5211DS18002W.

ABSTRACT Oil-paper insulation is the main insulating medium of converter transformers. Space charge can result in the distortion of electric field in oil-paper insulation, hence it's necessary to analyze the space charge transport characteristic and its influence on the oil-paper insulation. In the paper, the space charge transport characteristic considering the electric field is investigated, and an upstream finite element method is presented to calculate the space charge distribution in oil insulation of converter transformer considering the influence of injection barrier, ion mobility, trapped coefficient and carrier recombination coefficient. Finally, the insulation state of tortuous oil-path is evaluated. Experiments were conducted to analyze the relationship between ion mobility and electric field intensity, the results indicate that the influence of space charge on the electric field intensity in the tortuous oil-path can not be ignored for the design of converter transformer.

INDEX TERMS Electric field, ion mobility, space charge, converter transformer, upstream finite element.

I. INTRODUCTION

With the accumulation of space charge in converter transformer, the internal electric field would be distorted, finally the insulation breaks down and power accident arises. Therefore, it's necessary to investigate the space charge distribution considering the influence of electric field.

The experimental study is the main way to investigate the mechanism between the space charge and the electric field distribution in oil-paper insulation system [1]–[6]. Pulsed electro-acoustic (PEA) method was first proposed in 1983 [1], and used to conduct experiments to investigate the space charge distribution in 1997 [2]. Marie-Laure Locatelli et al used laser intensity modulation method (LIMM) [3] to study space charge formation under the electric field to address the mechanisms of space charge formation. Bu Wenbin et al used thermal stimulation depolarization current (TSDC) method [4] to investigated whether

the space charge distribution was affected by the internal electric field and potential distribution. Yuanwei Zhu, Shengtao Li, Daomin Min *et al.* used the pre-applied AC voltage method and the pre-applied DC voltage method to investigate the AC-DC combined voltage breakdown characteristics of one to four layers of oil impregnated paper insulation systemically, and discussed the space charge distributions and their electric field distortion in modulating AC-DC breakdown through numerical simulations [5]. Kai Wu, Qingdong Zhu, Haosen Wang *et al.* used the acoustic wave recovery method to study space charge distribution and distortion in oil insulation system [6]. However, due to the limitation of experiments conditions, these experimental studies mainly focused on the qualitative regularity of charge transport process, and didn't consider factors affecting the formation and the dissipation of space charge. Compared with experiments using methods such as PEA and LIMM, there also are some numerical simulation calculation methods [7]–[10]. Shengtao Li and Yuanwei Zhu studied the ac and dc breakdown strength respectively, and the space charge characteristic in these two

The associate editor coordinating the review of this manuscript and approving it for publication was Boxue Du.

conditions [7]. Zhifei Yang, Zhiye Du, Jiangjun Ruan, *et al.* used TUFEM to simulate the space charge motion in oil-paper insulation by the transient finite element method under considering the traps [8]. In addition, there are other studies about the space charge distribution considering different conditions in insulating materials [9], [10]. These results indicated that simulation and calculation could explain the mechanism better compared with experimental study. In addition, numerical simulation and calculation can analyze the mobility, and uniform distribution of space charge.

In terms of numerical simulation calculation, many scholars in the world have established some models. Most studies use the Poisson equation, current continuity equation and other relative equations to calculate the space charge distribution. In addition, in order to research the electric field distortion in the insulating material under the action of (direct current) DC voltage, most scholars mainly focus on the simulation calculation of the space charge distribution in the polyethylene of DC cable [11]–[13]. Alison *et al.* firstly proposed a bipolar space charge dynamic simulation model for space charge motion characteristics in cross-linked polyethylene materials in 1994 [11], but the study on polarity inversion voltage is still lacking. Based on the above model, Roy *et al.* optimized the model by using the method of Schottky electrode injection [12]. Zhou Yuanxiang added the Runge-Kutta discontinuous Galerkin method to Roy's space charge simulation model to obtain the process of space charge accumulation and dissipation of oil paper insulation material [13]. These models are based on the Poisson equation. However, because of the symmetry of the cable results, most models are based on one-dimensional analysis, so these models are not suitable for complex oil insulation structures of converter transformers such as oil insulation of converter transformers.

In this paper, the upstream finite element method has been proposed to work out the relationship between space charge and electric field distribution, and the model consisting injection barrier, carrier recombination, ion mobility, trapping, detrapping has been proposed. The result of this method shows that the space charge distribution is more complete under considering the non-uniform electric effect. In addition, the upstream finite element method can figure out the non-convergence problem of the final solution that is caused by the increase of the number of iterations in the calculation process. Besides, an experimental system has been constructed to obtain the nonlinear ion mobility under different electric field intensity. All work is divided into two parts, one part is experiment and the other part is numerical simulation.

II. EXPERIMENTAL SYSTEM

A. EXPERIMENTAL SETUP

The ion mobility of KI-50X insulating oil under different electric field intensity is measured. KI-50X insulating oil is

TABLE 1. Parameters of KI-50X insulating oil.

Physical properties	VALUE
Pour point	-51 C°
Density (20C°)	881 kg/m ³
Flash point	140 C°
Viscosity	15.8 mm ² /s
Breakdown voltage	88 kV
Interfacial tension	48 mN/m

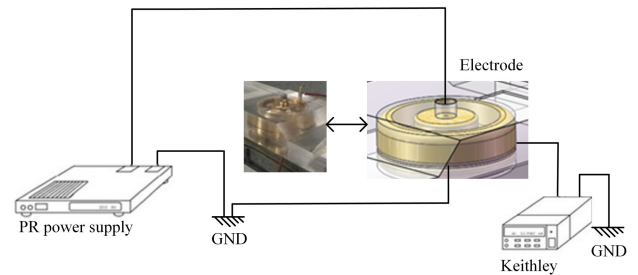


FIGURE 1. Modeling and physical diagrams of the experimental platform.

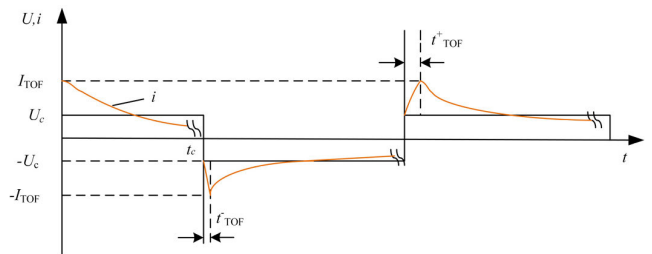


FIGURE 2. Polarity reversal voltage and measuring current.

always utilized in HVDC apparatus. High breakdown voltage and small dielectric loss factor can effectively prevent discharge and power loss under high voltage electric field, ensuring safe operation. The relative parameters are shown in the TABLE 1 [14].

The measurement platform is shown in FIGURE 1. The test of oil ion mobility is always measured by DC polarity reversal current [15].

B. ANALYSIS OF OIL MOBILITY

To investigate the relationship between oil mobility and electric field intensity, firstly, a polarity voltage U_c is applied, resulting in the ions randomly dispersed near the electrode surface, then a reversal voltage is applied after the duration $t = t_c$. Since the reverse time is far less than the migration time of ions, the ions accumulated around the electrode would migrate towards the electrode surface in the opposite direction. When the first batch of ions migrate to the test plate, the peak current arises, so the oil mobility can be calculated

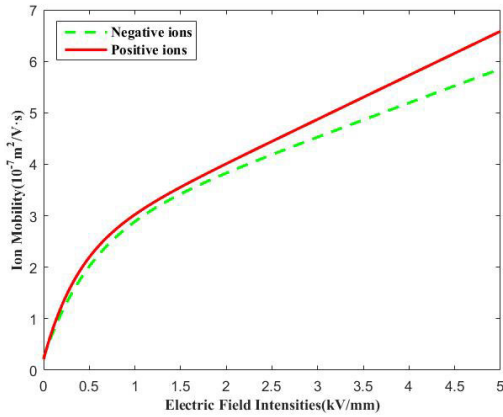


FIGURE 3. The relation between ion mobility and electric field intensity.

by the time of flight t_{tof} . Hence t_{tof} can be obtained according to the peak current I_{tof} of the transient current. The oil ion mobility under different field intensities are measured and the current change during the reversal polarity test is shown in FIGURE 2.

The ion mobility μ can be calculated as follows [16], [17].

$$\mu = \frac{d^2}{U_c t_{tof}} \quad (1)$$

where d is the gap distance between anode and the cathode, t_{tof} is the migration time, U_c is the polarity reversal voltage applied to the oil gap.

FIGURE 3 shows that the ion mobility grows exponentially with the electric field intensity within the field intensity range. Besides, the mobility of positive ions is slightly greater than the ion mobility of negative ions. At the beginning, the ion mobility increased rapidly with the electric field intensity. When the electric field intensity reaches 0.52 kV/mm, the rate of increase of the ion mobility would be slow down and tends to be saturated once the electric field intensity reaches a certain value.

Therefore, it is necessary to research the electric field intensity in the tortuous oil-path to the space charge distribution. In the next step, the study of numerical simulation will be carried out.

III. METHOD

A. THE UPSTREAM FINITE ELEMENT

To calculate the space charge density and electric field intensity with the method of upstream FEM, the upstream element should be determined in the iterative computation, and FIGURE 4 shows the way to hunt for upstream FEM elements.

If the charge density of the point m is obtained from the known charge density of the point i and the point j , it is necessary to judge whether or not the triangle ijm associated with m constitutes the upstream element. Turn counterclockwise, the next point of node m is defined as i , and the second point

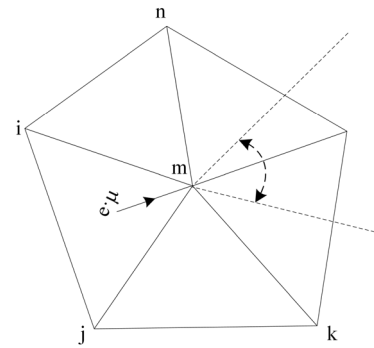


FIGURE 4. The judgment of upstream finite element.

is defined as j . The vectors b and c are obtained by rotating the vectors jm and im counterclockwise by 90° respectively. If the angle between the space charge migration velocity $e \cdot \mu$ of the point m and the vector $-b$ and c are both less than 90° , the triangular element is an upstream element. Then, solve the charge density of a node in each upstream element. Similar to the method of interpolating potentials when solving the Poisson equation, interpolating the charge density in the triangle ijm (2-3) [18], [19].

$$\rho(x, y) = N_i \rho_i + N_j \rho_j + N_m \rho_m = [N] [\rho] \quad (2)$$

The N_i , N_j and N_m satisfy the equation (3):

$$N_i + N_j + N_m = 1 \quad (3)$$

The partial derivative of the coordinates is shown as (4-5):

$$\frac{\partial \rho}{\partial x} = \left[\frac{\partial N}{\partial x} \right] [\rho] = \frac{1}{2\Delta} (b_i \quad b_j \quad b_m) [\rho] \quad (4)$$

$$\frac{\partial \rho}{\partial y} = \left[\frac{\partial N}{\partial y} \right] [\rho] = \frac{1}{2\Delta} (c_i \quad c_j \quad c_m) [\rho] \quad (5)$$

where ρ represents the charge density, Δ is the area of the upstream element.

In addition, as the number of iterations increases during the calculation process, the calculation error is also continuously accumulated, resulting in non-convergence of the final solution. To solve this problem, the upstream finite element [20]–[22] is adopted in this paper, in which the space charge density is calculated by sweeping along the axis direction of the oil channel of the transformer [18], and the update direction is bidirectional. In addition, the updated way of charge density of the upstream finite element is shown in FIGURE 5.

B. BIPOLAR TRANSPORT MODEL

For the charge injection of the electrodes, Schottky injection is used as the only source of charge in the medium [23], and the carrier on the surface of the electrode is influenced by the electric field, the temperature and the injection

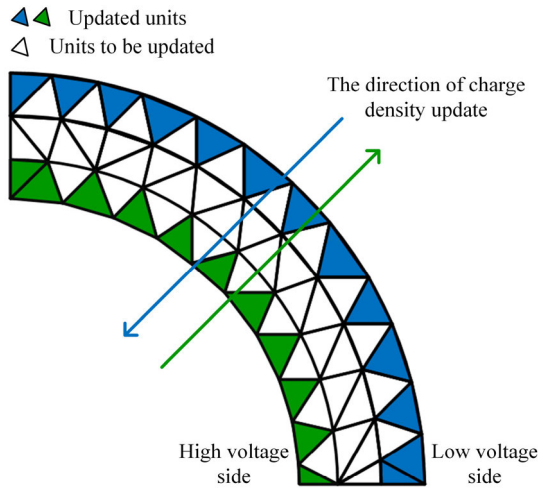


FIGURE 5. The updated way of charge density.

barrier [24], [25].

$$J_e = AT^2 \exp\left(-\frac{e\omega_{ei}}{kT}\right) \exp\left(\frac{e}{kT} \sqrt{\frac{e|E_C|}{4\pi\epsilon}}\right) \quad (6)$$

$$J_h = AT^2 \exp\left(-\frac{e\omega_{hi}}{kT}\right) \exp\left(\frac{e}{kT} \sqrt{\frac{e|E_a|}{4\pi\epsilon}}\right) \quad (7)$$

where A is the Richardson constant which is $1.2 \times 10^6 \text{ A}/(\text{m}^2\text{K}^2)$, T is the thermodynamic temperature, k is the Planck constant. J_h and J_e are respectively the hole density injected from the cathode and the electron current density injected from the anode. E_C and E_a represent the surface average electric field intensity of the cathode and the anode. ω_{ei} and ω_{hi} are the injection barrier of the cathode and anode surfaces respectively.

Owing to the traps inside the oil insulation medium, free electrons and free holes are captured in motion, resulting the trapped electrons and trapped holes [26]. Therefore, four kinds of carriers exist in the medium including free electrons (eu), free holes (hu), trapped electrons (et) and trapped holes (ht), and the carriers will combine each other during the motion. In addition, n represents the carrier density.

The net charge density n_0 in the medium is defined as the origin of the charge densities of the four carriers, which is shown in (8), and the positive or negative value of the net charge density depends on the polarity and charge of four carriers.

$$n_0 = n_{ht} + n_{hu} - n_{eu} - n_{et} \quad (8)$$

In order to describe trapping and recombination process of the carrier, four carrier source terms are represented by S_{eu} , S_{et} , S_{hu} , S_{ht} . In addition, the transport model of four types of carrier are shown as (9-12).

$$S_{eu} = -eB_{eu,ht}n_{eu}n_{ht} - eB_{eu,hu}n_{eu}n_{hu} - B_e n_{eu} \left(1 - \frac{en_{et}}{N_{et0}}\right) \quad (9)$$

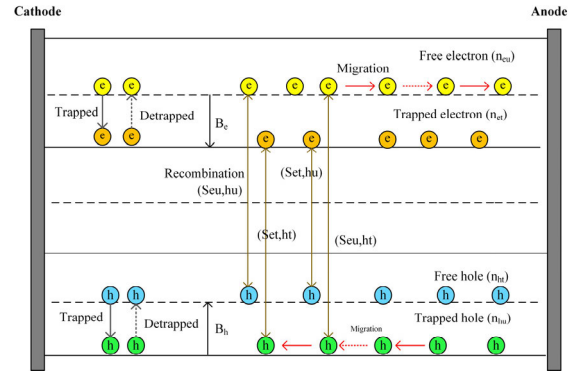


FIGURE 6. The recombination, trapping, detrapping, migration of carriers.

$$S_{et} = -eB_{et,hu}n_{et}n_{hu} - eB_{et,ht}n_{et}n_{ht} - B_e n_{eu} \left(1 - \frac{en_{et}}{N_{et0}}\right) \quad (10)$$

$$S_{hu} = -eB_{et,hu}n_{et}n_{hu} - eB_{eu,hu}n_{eu}n_{hu} - B_h n_{hu} \left(1 - \frac{en_{ht}}{N_{ht0}}\right) \quad (11)$$

$$S_{ht} = -eB_{eu,ht}n_{eu}n_{ht} - eB_{et,ht}n_{et}n_{ht} - B_h n_{hu} \left(1 - \frac{en_{ht}}{N_{ht0}}\right) \quad (12)$$

where $B_{eu,hu}$, $B_{et,hu}$, $B_{et,ht}$, $B_{eu,ht}$ are the composite coefficients between each of the two carriers, B_e and B_h are respectively the recombination coefficients of electrons and holes. N_{et0} , N_{ht0} are the trap concentration of electrons and holes.

The diagram of the entire carrier transport model is shown in FIGURE 6 [27], [9]. In the figure, ions would migrate, and the ion mobility changes with the electric field intensity.

C. CHARGE TRANSFORMATION MODEL UNDER THE ELECTRIC FIELD

Equations (13-15) contain the Poisson's equation and current continuity theorem. The Poisson's equation (13) is used to calculate the electric field of space charges. The convection-reaction equation (14) shows the charge density updated in every iteration step. The mass conservation equation (15) reflects the mass transformation including migration [28].

$$\nabla^2 \varphi = \frac{\rho}{\epsilon} \quad (13)$$

$$R_i \frac{\rho}{e} + \nabla j = 0 \quad (14)$$

$$j = u \cdot \rho \cdot E \quad (15)$$

where e is the elementary charge, R_i is the recombination coefficient of four types of carriers, j is the current density, μ is the ion mobility, ρ is the space charge density.

D. FLOW CHART

Firstly, the Poisson equation would be solved. Next, the upstream element information of each node is gained. Then, computation starting from the upper and lower boundaries

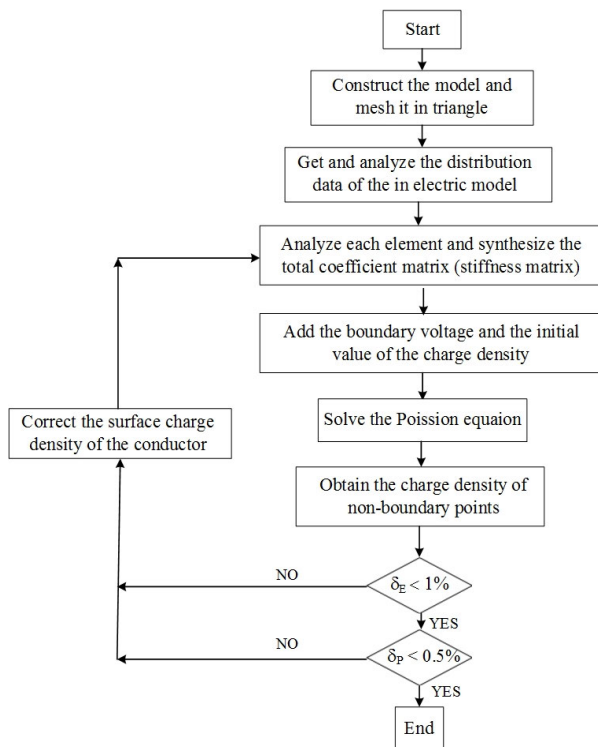


FIGURE 7. Flow chart of the upstream FEM.

and sweep to the other side at the same time. If an element composed of two nodes with known charge density and this element is the upstream element of the third node, then the calculation is proceeding. Finally, this step would be repeated until the charge density at each point is calculated. So far, the reverse calculation of the space charge density from the potential distribution is completed. The process is shown in FIGURE 7.

IV. MATHEMATICAL MODEL

In this paper, the tortuous oil-path is taken as the analysis model. In addition, the model is meshed in 198 elements and 127 nodes.

For the parameter setting in the tortuous oil-path of the oil-filled transformer. The parameters of oil insulation are set as shown in TABLE 2.

V. RESULTS

Based on the experiment, the variable ion mobility increases with electric field. In order to analyze the relationship between distribution of space charge density and electric field intensity in the tortuous oil-path more accurately, three blue lines in figure 8 have been adopted as sample lines. In this paper, two cases are considered. Condition 1 considers the ion mobility that varies with the electric field intensity, and condition 2 considered the constant ion mobility which would not change with the electric field intensity.

Take sample line 1 and sample line 3 for analyze, just as shown in FIGURE 9 and 10, because the variable ion mobility

TABLE 2. Parameters.

Symbol	Quantity	Value and units
B_e	Trapping coefficient of electrons	5×10^{-3} (/s)
B_h	Trapping coefficient of holes	5×10^{-3} (/s)
$B_{ef,hf}$	The recombination coefficient of free electrons/free holes	5×10^{-3} (/m ³ *C*s)
$B_{ef,ht}$	The recombination coefficient of free electrons/trapped holes	1×10^{-3} (/m ³ *C*s)
$B_{et,hf}$	The recombination coefficient of trapped electrons/free holes	1×10^{-3} (/m ³ *C*s)
$B_{et,ht}$	The recombination coefficient of trapped electrons/trapped holes	0 (/m ³ *C*s)
$N_{t,e}$	Trap concentration of electrons	100 (C/m ³)
$N_{t,h}$	Trap concentration of holes	100 (C/m ³)
ω_{ei}	The injection barriers of electrons	1.1 (eV)
ω_{hi}	The injection barriers of holes	1.1 (eV)
ϵ_r	Relative dielectric constant	2.2

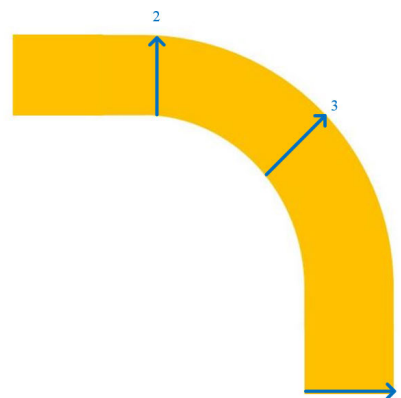


FIGURE 8. The sample lines in the tortuous oil-path.

TABLE 3. Parameters of KI-50X insulating oil.

Different conditions	The maximum charge density (C/m ²)
Condition 1	-10.0354
Condition 2	-15.6766

under the electric field intensity is greater than the constant ion mobility, the phenomenon of ion trapping around the electrode would be reduced. Therefore, for the same line, the space charge density with variable ion mobility is always smaller than the constant ion mobility's.

After considering the electric field intensity, the space charge density decreases by 5.6214C/m². The TABLE 3 shows the maximum charge density in two conditions.

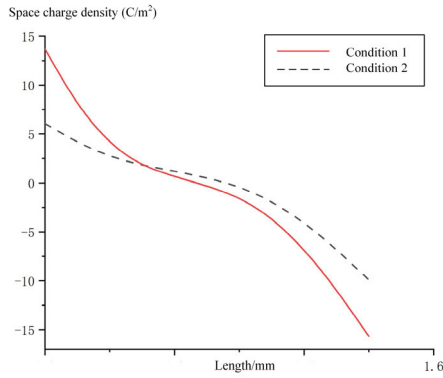


FIGURE 9. The line chart of the space charge distribution in two conditions on the sample line 1.

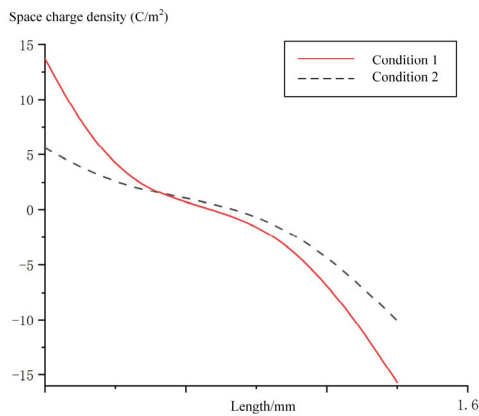


FIGURE 10. The line chart of the space charge distribution in two conditions on the sample line 3.

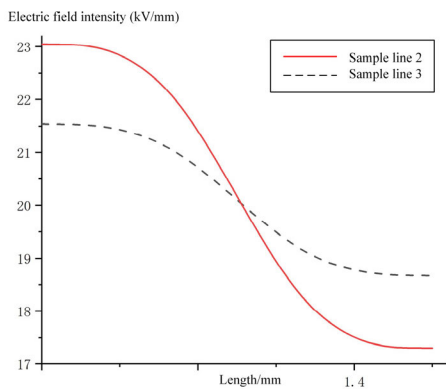


FIGURE 11. The electric field intensity distribution in two conditions.

According to FIGURE 11, as the sample line moves from the middle of the ring to the rectangle at both ends, the electric field intensity would gradually decrease, and the decaying rate of electric field intensity in the edge of sample line is smaller. The high electrode side of the bending path has a large curvature radius, resulting in the charge accumulate intensively and the electric field intensity largely; while in the straight path, owing to smaller curvature radius, the charge distribution is dispersed and the electric field intensity is

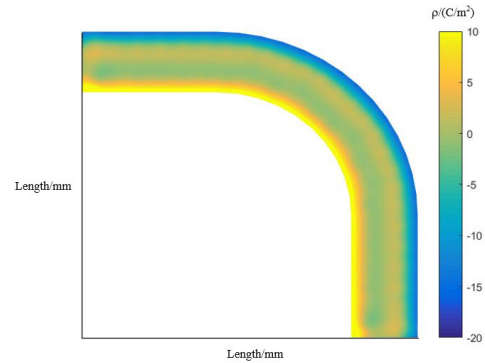


FIGURE 12. The space charge distribution in tortuous oil-path with the ion mobility.

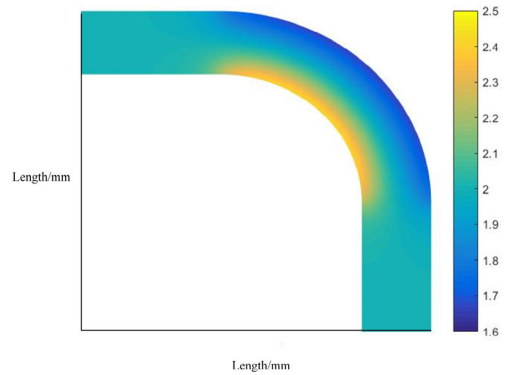


FIGURE 13. The electric field intensity distribution in the tortuous oil-path.

small. Thus, the maximum electric field intensity exists near the high electrode of the bending path. In addition, according to the space charge density distribution figure, the electric field distortion is mainly caused by the accumulation of space charge.

FIGURE 12 shows the space charge distribution in the tortuous oil-path with the variable ion mobility. Due to the effect of the electric field, the space charge would migrate, so the electrons and holes inside the tortuous oil-path would more easily migrate to the electrode. Since the electrons and holes inside the tortuous oil-path are more likely to migrate and recombine with charges of opposite polarity, and the internal space charge distribution is relatively less. Therefore, when dynamic equilibrium is reached, many charges with the same polarity would accumulate near the plates. However, because of the influence of electric field, the space charge distribution would change, so the actual situation is closer to FIGURE 12 (b).

As shown in FIGURE 13, it's the electric field distribution contour. In addition, the peak value appears near the anode, and the electric field intensity reaches 2.3047×10^7 V/m. While, the minimum electric field intensity is near the cathode, which is 1.7298×10^7 V/m. The electric field intensity distribution is characterized by “high on the anode and low on the cathode”. According to the space charge distribution

diagram, the electric field distortion is mainly caused by the accumulation of space charge.

VI. CONCLUSIONS

The oil-immersed power transformer is one of the main equipment in the power system, and its internal space charge distribution is one of the issues that need to be paid attention during the design of the transformer. This paper studies the influence of electric field on space charge of oil-immersed transformer. In addition, conclusions contain the experiment and the numerical simulation.

- 1) The experiment shows the ion mobility increasing with the electric field intensity. In addition, after considering the electric field intensity, the space charge density decreases by 5.6214C/m^2 .
- 2) Simulation results show that many charges with the same polarity accumulate near the electrode, and the electric field intensity reaches to the highest value at the bending area of anode.
- 3) The calculation result verifies that the presence of the electric field obviously affects the internal space charge distribution of the oil insulation in converter transformers.
- 4) The electric field intensity distribution in the tortuous oil-path is characterized by “high on the anode and low on the cathode”, and the electric field distortion is mainly caused by the accumulation of space charge.

REFERENCES

- [1] T. Takada and T. Sakai, “Measurement of electric fields at a dielectric/electrode interface using an acoustic transducer technique,” *IEEE Trans. Electr. Insul.*, vol. EI-18, no. 6, pp. 619–628, Dec. 1983.
- [2] P. Morshuis and M. Jeroense, “Space charge measurements on impregnated paper: A review of the PEA method and a discussion of results,” *IEEE Elect. Insul. Mag.*, vol. 13, no. 3, pp. 26–35, May 1997.
- [3] M.-L. Locatelli, C. D. Pham, S. Diahm, L. Berquez, D. Marty-Dessus, and G. Teyssedre, “Space charge formation in polyimide films and polyimide/SiO₂ double-layer measured by LIMM,” *IEEE Trans. Dielectr. Electr. Insul.*, vol. 24, no. 2, pp. 1220–1228, Apr. 2017.
- [4] W. Bu, J. Yin, F. Tian, and Q. Lei, “Numerical analysis of space charge electric field and its effect on TSDC measurement in thin polymer films,” presented at the IEEE 9th Int. Conf. Properties Appl. Dielectr. Mater., Jul. 2009.
- [5] Y. Zhu, S. Li, D. Min, S. Li, H. Cui, and G. Chen, “Space charge modulated electrical breakdown of oil impregnated paper insulation subjected to AC-DC combined voltages,” *Energies*, vol. 11, no. 6, p. 1547, Jun. 2018.
- [6] K. Wu, Q. Zhu, H. Wang, X. Wang, and S. Li, “Space charge behavior in the sample with two layers of oil-immersed-paper and oil,” *IEEE Trans. Dielectr. Electr. Insul.*, vol. 21, no. 4, pp. 1857–1865, Aug. 2014.
- [7] S. Li, Y. Zhu, D. Min, and G. Chen, “Space charge modulated electrical breakdown,” *Sci. Rep.*, vol. 6, no. 1, p. 32588, Dec. 2016, doi: 10.1038/srep32588.
- [8] Z. Yang, Z. Du, J. Ruan, S. Jin, G. Huang, Q. Lian, and Y. Liao, “Simulation on motion characteristics of space charge in single oil-paper insulation,” *COMPEL-Int. J. Comput. Math. Electr. Electron. Eng.*, vol. 36, no. 6, pp. 1663–1675, Nov. 2017.
- [9] D. Min and S. Li, “A comparison of numerical methods for charge transport simulation in insulating materials,” *IEEE Trans. Dielectr. Electr. Insul.*, vol. 20, no. 3, pp. 955–964, Jun. 2013.
- [10] Q. Zhu, X. Wang, K. Wu, Y. Cheng, Z. Lv, and H. Wang, “Space charge distribution in oil impregnated papers under temperature gradient,” *IEEE Trans. Dielectr. Electr. Insul.*, vol. 22, no. 1, pp. 142–151, Feb. 2015.
- [11] J. M. Alison and R. M. Hill, “A model for bipolar charge transport, trapping and recombination in degassed crosslinked polyethylene,” *J. Phys. D, Appl. Phys.*, vol. 27, no. 6, pp. 1291–1299, Jun. 1994.
- [12] S. L. Roy, G. Teyssedre, and C. Laurent, “Modelling space charge in a cable geometry,” *IEEE Trans. Dielectr. Electr. Insul.*, vol. 23, no. 4, pp. 2361–2367, Aug. 2016.
- [13] J. Tian, Y. Zhou, and Y. Wang, “Simulation of space charge dynamics in low-density polyethylene under external electric field and injection barrier heights using discontinuous Galerkin method,” *IEEE Trans. Dielectr. Electr. Insul.*, vol. 18, no. 5, pp. 1374–1382, Oct. 2011.
- [14] (2012). *Material Safety Data Sheet of the KI-50X Insulating Oil of the DC Transformer*. [Online]. Available: <http://kunlunlube.cnpc.com.cn/klrhy/msdstzy/201606/ta791152f8794a6199c7ba19fa8cfd7f/files/1740388a6a3d42e69e033aa95a89db5e.pdf>
- [15] R. Tobazeon, J. C. Filippini, and C. Marteau, “On the measurement of the conductivity of highly insulating liquids,” *IEEE Trans. Dielectr. Electr. Insul.*, vol. 1, no. 6, pp. 1000–1004, Dec. 1994.
- [16] B. Dikarev, G. Karasev, R. Romanets, and N. Shimon, “Modelling and experimental research of the non-stationary processes of conduction and space charge accumulation in dielectric liquids,” in *Proc. IEEE 13th Int. Conf. Dielectr. Liquids (ICDL)*, Jul. 1999, pp. 33–36.
- [17] M. Watanabe, S. Nagano, K. Sanui, and N. Ogata, “Ionic conductivity of network polymers from Poly(ethylene oxide) containing lithium perchlorate,” *Polym. J.*, vol. 18, no. 11, pp. 809–817, Nov. 1986.
- [18] Y. Feng, “Calculation of synthetic field strength and ion current density under HVDC transmission line,” China Electr. Power Res. Inst., Beijing, China, Tech. Rep. TM714, 1998. [Online]. Available: http://www.wanfangdata.com.cn/details/detail.do?_type=degree&id=Y308205
- [19] W. Xuewan, “Numerical calculation of ion flow field in HVDC transmission line,” China Electr. Power Res. Inst., Beijing, China, Tech. Rep. TM726.1, 1989. [Online]. Available: http://www.wanfangdata.com.cn/details/detail.do?_type=degree&id=Y063464
- [20] T. Takuma, T. Ikeda, and T. Kawamoto, “Calculation of ION flow fields of HVDC transmission lines by the finite element method,” *IEEE Trans. Power App. Syst.*, vol. PAS-100, no. 12, pp. 4802–4810, Dec. 1981.
- [21] Z. Du, G. Huang, J. Ruan, G. Wang, Y. Yao, C. Liao, J. Yuan, and W. Wen, “Calculation of the ionized field around the DC voltage divider,” *IEEE Trans. Magn.*, vol. 49, no. 5, pp. 1933–1936, May 2013.
- [22] G. D. Huang, J. J. Ruan, Z. Y. Du, C. B. Liao, S. Jin, and G. L. Wang, “Improved 3-D upwind FEM for solving ionized field of HVDC transmission lines,” *Proc. CSEE*, vol. 33, pp. 152–159, Nov. 2013.
- [23] S. L. Roy, P. Segur, G. Teyssedre, and C. Laurent, “Description of bipolar charge transport in polyethylene using a fluid model with a constant mobility: Model prediction,” *J. Phys. D, Appl. Phys.*, vol. 37, no. 2, pp. 298–305, Jan. 2004.
- [24] Y. Li, F. He, and C. Liu, “Two-dimensional geometry effect on space-charge-limited current in axially symmetrical planar diode,” *High Power Laser Part. Beams*, vol. 17, no. 6, pp. 913–916, 2005.
- [25] Z. Yinghong, W. Jianguo, Z. Jinhui, N. Shengli, and F. Ruyi, “Influence of temperature effect of field emission on explosive electron emission in microwave tube,” *High Power Laser Part. Beams*, vol. 25, no. 5, pp. 1236–1239, 2013.
- [26] S. Jin, J. Ruan, Z. Du, Z. Yang, T. Zhou, G. Huang, and L. Zhu, “Charge transport in oil impregnated paper insulation under temperature gradient using transient upstream FEM,” *CSEE J. Power Energy Syst.*, vol. 1, no. 3, pp. 3–8, Sep. 2015.
- [27] D. Min, W. Wang, and S. Li, “Numerical analysis of space charge accumulation and conduction properties in LDPE nanodielectrics,” *IEEE Trans. Dielectr. Electr. Insul.*, vol. 22, no. 3, pp. 1483–1491, Jun. 2015.
- [28] H. Liu, R. Liao, Q. Zhu, X. Zhao, K. Liu, and X. Li, “Calculation of space charge density in negative corona based on finite-element iteration and sound pulse method,” *IEEE Trans. Magn.*, vol. 54, no. 3, pp. 1–4, Mar. 2018.



ZHAOXIANG ZHANG was born in Hunan, China, in 1999. He is currently pursuing the B.E. degree with the School of Electrical Engineering, Chongqing University—University of Cincinnati Joint Co-op Institute, Chongqing University, Chongqing, China. His research interests include multi-physics coupling field calculation and electromagnetic numerical calculation.



KAI YANG was born in Jiangxi, China, in 1999. He is currently pursuing the B.E. degree with the Chongqing University—University of Cincinnati Joint Co-op Institute, School of Electrical Engineering, Chongqing University, Chongqing, China. His research interests include multi-physics coupling field calculation and electromagnetic numeral calculation.



LI LIU received the master's degree from the School of Electrical Engineering, Chongqing University, China, in 2003. He is currently the Deputy Director of the Apparatus Condition Evaluation Center of State Grid Zhejiang Electric Power Company. His research interests include condition monitoring methods for electrical apparatus and the multi-physics coupling field calculation for electrical apparatus.



CHENG CHI received the B.E. degree from the School of Electrical Engineering, North China Electric Power University. She is currently pursuing the Ph.D. degree with the School of Electrical Engineering, Chongqing University, Chongqing, China. Her research interests include multi-physics coupling field calculation and electromagnetic numeral calculation.



FAN YANG (Member, IEEE) received the Ph.D. degree from the School of Electrical Engineering, Chongqing University, China, in 2008. He was a Visiting Scholar at Oklahoma State University, OK, USA, in 2012. He is currently a Professor of electrical engineering at Chongqing University. His research interests include condition monitoring methods for electrical apparatus and the multi-physics coupling field calculation for renewable devices.



SHAOHUA WANG (Member, IEEE) received the Ph.D. degree from the School of Electrical Engineering, Chongqing University, China, in 2008. He is mainly engaged in the status detection and evaluation of power transmission and transformation equipment.

...